Compact phased arrays for microseismic monitoring

Paul A. Nyffenegger[1*], Mark A. Tinker[1], Jian Zhang[1], Elige B. Grant[1], Kevin D. Hutchenson[1] and Don C. Lawton[2] demonstrate the promising performance of permanently deployed, networked SADAR arrays to detect and locate microseismicity associated to CO_2 storage reservoirs.

Abstract

A network of four SADAR® arrays installed at Carbon Management Canada's (CMC) Containment and Monitoring Institute (CaMI) Field Research Station provides an example of the results achievable through passive monitoring of microseismicity at an active CO_2 storage facility. The SADAR arrays, designed as compact volumetric phased arrays, provide a passive, persistent, and permanent data acquisition and analysis capability. Data from compact phased arrays are processed to take advantage of the spatial coherence of the incident seismic signals to increase signal resolution while suppressing noise and clutter signals, and simultaneously providing signal attributes such as angle-of-incidence and phase velocity. The network of arrays allows for automation of location and magnitude determination at a reduced channel count and sensor footprint. We present results from a nine-day reporting period, a subset of the overall compiled seismic event bulletin, chosen because the time span contains both CO_2 injection events as well as other non-injection activities. A total of 55 events were detected and located with an M_w = -2.5 threshold. The results demonstrate the promising performance of permanently deployed, networked SADAR arrays to detect and locate microseismicity associated with CO_2 storage reservoirs. Technologies such as SADAR will be an enabling driver as industries embark upon gigatonne storage capacities.

Introduction

For transformation of the energy industry and achieving large-scale net-emission reductions, capture and storage of CO_2 tens of gigatons will be required. Economical and effective measurement, monitoring, and verification (MMV) technologies help to manage the risks associated with underground carbon sequestration, ensure ongoing operations, and verify reservoir integrity. One key technology is passive seismic monitoring for the sensing and characterization of micro-earthquakes associated with CO_2 injection, operations, or failure. At the gigatonne storage level, passive seismic systems face the challenge of providing useful information in real time as well as being cost effective, permanent, and maintainable.

Quantum Technology Sciences' (Quantum's) SADAR system uses passive underground phased arrays permanently deployed in the shallow subsurface for enhancing the signal-to-noise ratio and reducing clutter through spatial filtering. Additionally, the data processing workflow lends itself to automation and real-time reporting as well as customized reservoir analytics based on the accumulated information. In comparison with other seismic deployments, SADAR arrays offer a reduced surface footprint, enhanced signal detection capabilities, and a more complete understanding of the incident seismic signals. Passive, persistent, permanent seismic monitoring using compact phased arrays can be automated to observe patterns of seismicity in the reservoir horizon and surrounding geologic units and can deliver this information in real time as the activity is unfolding.

Background

Historically, seismic monitoring has focused mostly on detection and characterization of impulsive transient (IT) signals originating from earthquakes and underground nuclear explosions; i.e., short duration, broadband signals. In comparison, passive undersea monitoring or atmospheric monitoring has an expanded signal set that includes tones of extended duration, known as continuous waveform (CW) signals, or frequency modulated waveforms (FM) generated by a variety of sources including motorized watercraft and aircraft.

As has been documented in numerous studies, any of these signals propagating through the atmosphere or through the oceans can be acquired to some extent using seismic apparatus. However, these types of signals are considered noise for typical installations of seismic instruments. Furthermore, the majority of these types of signals occur at frequencies generally above 10 Hz and the primary frequency band of interest for most passive seismic monitoring systems. Lastly, seismic sensors deployed on the surface, in post holes, or in shallow vaults are particularly susceptible to these other 'noise' signals.

For global nuclear test ban treaty monitoring both very large aperture seismic arrays designed for teleseismic monitoring and smaller aperture arrays designed for regional monitoring have been integrated into the monitoring networks (see 'Forensic Seismology and Nuclear Test Ban Treaties' by Douglas (2013) for a review). The largest of these arrays were designed with apertures greater than 100 km whereas regional array designs have apertures of several kilometres to ~ 25 km and usually include ~15-25 elements. Planar or two dimensional (2D) arrays for global monitoring were often designed as combinations of uniform linear arrays, deployed approximately orthogonally, with a few others designed as concentric uniform circular arrays. Regardless of the arrangement of array elements, the goal of fielding an array is to apply coherent

[1] Quantum Technology Sciences, Inc. (Quantum) | [2] Carbon Management Canada
* Corresponding author, E-mail: pnyffenegger@qtsi.com
DOI: 10.3997/1365-2397.fb2022033

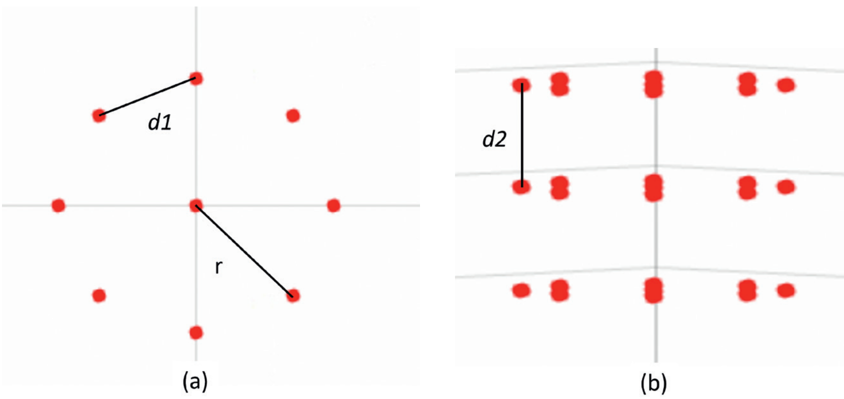

Figure 1 A basic compact volumetric array shown in map view (a) and vertical cross-section (b). The chosen design in this example is a uniform cylindrical array of radius r having a central column, with element spacing *d1* within a sensor layer and *d2* between sensor layers.

processing to the collected data to increase the coherent signal relative to the noise and provide an assessment of the direction of arrival of the signal.

As used in this context, coherent processing means spatially-coherent processing, i.e. beamforming, where signals acquired with multiple geometrically arranged point sensors (an array) are cooperatively processed based on the coherence of signals propagating across the array to create a beam, which is pointed outwards from a defined reference point along a main response axis (MRA). When the beam MRA is aligned with the signal angle of incidence, the signal power is maximized, and the non-coherent noise power is minimized. The term 'point sensor' means the dimensions of the sensor are much smaller than the wavelength of the maximum seismic frequency of interest, i.e. as a sensor that measures the applicable field at a single point, rather than as a distributed sensor that integrates signal measurements over a finite aperture. 'Point sensors' are also referred to as array elements, and may be single sensors, or multiple vector sensors as is the case with elements composed of triaxial geophone packages.

Since 2005, Quantum has created, assembled, and marketed patented and patent-pending systems for security, surveillance, and industrial monitoring applications (e.g., Nyffenegger et al., 2015; Davis et al., 2015; Davis et al., 2017; Tinker et al., 2019; and Tinker et al., 2021). These systems include SADAR 2-dimensional arrays designed to monitor IT, CW, and FM signals in the frequency band extending from a few Hz to a few kHz. For more than five years, Quantum has been developing and deploying the data acquisition hardware and analytic software systems for real-time subsurface monitoring using compact volumetric (three dimensional) SADAR arrays.

A primary reason for the term 'compact array' is to distinguish these systems from extended linear or planar sensor deployments, or combinations of extended linear and planar sensor deployments of significant channel count. As an example, the geometry of a basic compact volumetric phased array is shown in Figure 1, designed specifically as a uniform cylindrical array with a central column. The element spacing, *d*, depends on the design frequency f_d of the array. The corresponding design wavelength is $\lambda_d = c/f_d$ where *c* is the phase velocity of the media where the array is emplaced. Ideally the element spacings *d* are derived from the design wavelength as $d = \lambda_d/2$. Because seismic propagation involves multiple wave modes travelling at different phase velocities *c*, an array with a single element spacing *d* will correspond to more than one design wavelength. The uniform cylindrical array of Figure 1 takes advantage of two design frequencies, yielding two element spacings, *d1* and *d2* for the P waves (in this example), and providing an overall broader band array response pattern.

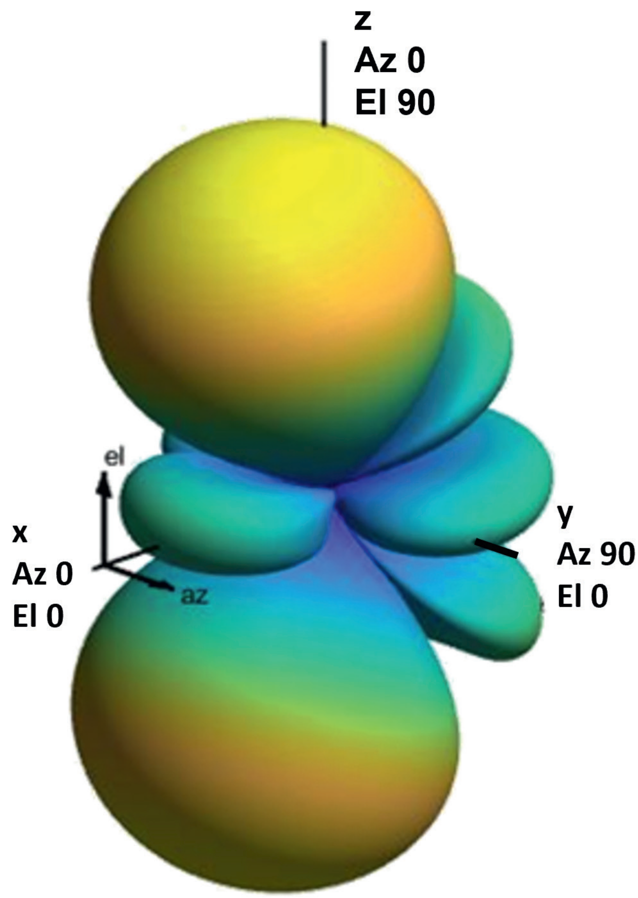

Figure 2 Calculated beam response pattern for the basic compact volumetric array shown in Figure 1. This response is for angle of arrival azimuth=0 degrees, dip=70 degrees, and signal frequency f=0.75f_d.

Array response patterns for 2D arrays, including linear arrays, are commonly shown in plots resembling antenna patterns, or else as wavenumber responses, as a function of both frequency and signal angle of incidence (e.g. Havskov and Alguacil, 2006; Schweitzer et al., 2012; Douglas, 2013). Volumetric array response patterns are inherently more complicated than those for 2D arrays. As shown in Figure 2, the array response pattern in three dimensions for a uniform cylindrical array with a central column appears as a complex volume that is a function of the propagating signal's angle of incidence as well as frequency. The pattern is given for a single frequency, close to the design frequency, and the signals of interest for this case are broadband impulsive transients.

The data analysis system components for local SADAR arrays typically operate in layered sequential stages in multiple, parallel processing pipelines, customized to the nature of the signals of interest. These automated processing pipelines are constructed in a common architecture known as 'Detect-Classify-Localize-Track' or DCLT (e.g. Abraham, 2019). Signal analysis pipeline components including joint-attribute-time analysis occurs to a large extent on data collected from single arrays, with 'localize and track' processing performed almost exclusively on a network basis. In the most advanced stages, the processing pipelines govern fusion algorithms operating over time, space, and derived attributes to identify a source class, localize the source, spatially track the source, and provide that information to system operators through a GIS-based user interface.

Data

The data used in this study were recorded from Carbon Management Canada's Containment and Monitoring Institute's (CaMI) Field Research Station CO_2 injection site. At this site, small volumes of CO_2 are being injected at a depth of 300 m, simulating an upward leakage of CO_2 from a deeper storage reservoir (Lawton, et al., 2019). Goals of the facility include determining the detection threshold of CO_2 using a broad array of monitoring technologies (Macquet et al., 2019) and investigating the advantages of continuous microseismic monitoring. A network of four permanent arrays installed at the site in 2021 provides persistent monitoring of the reservoir and surrounding geology. The goal of the deployment is to evaluate array performance in terms of signal-to-noise ratio (SNR) gain and spatial accuracy as well as probability of detection (P(d)) as a function of range and source level. These metrics will be carried into an understanding of network performance in terms of location accuracies and uncertainties.

This paper presents the subset of results covering a 9-day period of the recording of the CaMI site. During that time, two injections of CO_2 occurred into the reservoir. The SADAR arrays comprise Geospace GS-ONE 10 Hz vertical sensors for array elements, each sensor attached to a dedicated 24-bit digitizer set at 2000 samples per second. In order to ensure synchronized timing across all the arrays/elements, all data acquisition and logging is coordinated through a single Geospace GeoRes System with a GPS time source.

The four arrays were installed at distances that ranged between 70 and 300 m from the injection well and at depths ~10 m below ground surface to the uppermost sensors (Figure 3). Two cylindrical-like array designs were tested with variations in aperture and layers and consisted of two 9-column, 6-level (54 sensors) arrays, one 17-column, 3-level (51 sensors) array, and one 17-column, 6-level (72 sensors) array, which was designed to be a hybrid of the first two designs. The deployed arrays are designed as oversized, allowing for array subsets to be evaluated for performance and effectiveness.

Phased array analysis

Quantum employs both standard and proprietary phased-array data processing techniques to extract information from seismic waveforms. For example, information provided by the analysis includes angle of incidence and true phase velocity of that energy as it propagates across the array. For the automated SADAR systems, the array processing begins with beamforming over four dimensions – azimuth, dip, true phase velocity across the array, and frequency – for a given time frame. This information is used to create the optimally oriented beam that maximizes the coherent signal arriving along that beam MRA, minimizes non-coherent noise, and also minimizes coherent signals incident upon the array from other directions. When combined with other noise suppression techniques, coherent processing reduces the uncertainty in determining seismic arrivals and the type of energy

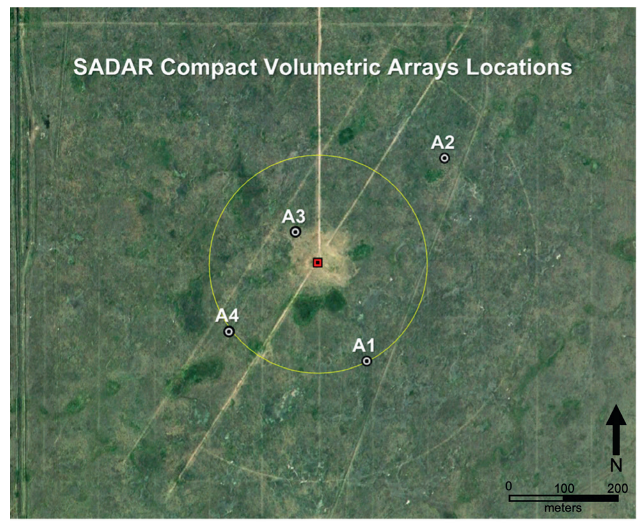

Figure 3 A map view showing the injection well (red square) and four SADAR arrays. The yellow circle represents 200 m from the injection well.

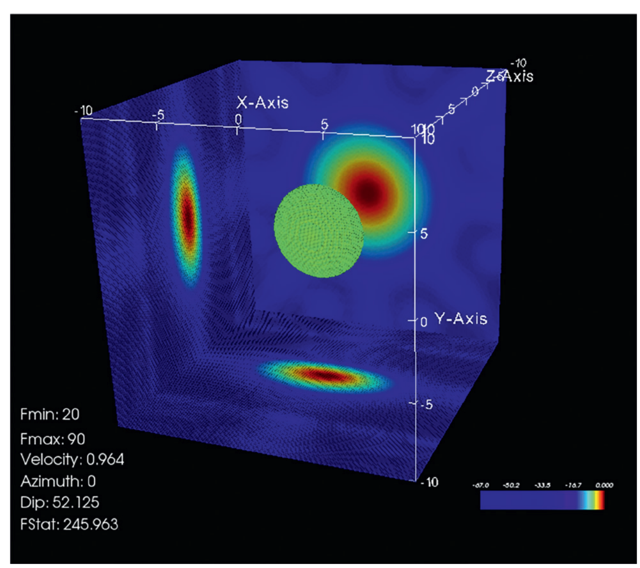

Figure 4 Three-dimensional frequency-wavenumber (FK) analysis for the subsurface event shown in Figure 5 as recorded on A1. This illustrates the 3D slowness domain, projected onto cartesian slowness space in units of seconds/kilometre (x,y,z axis). The optimal slowness vector in spherical coordinates converts to velocity, azimuth, and dip as shown in the annotation in the lower left. The optimal slowness vector maximizes the integrated signal power for the FK pattern over the band of 20-90 Hz and a time frame of 0.15 seconds. The green sphere illustrates 10dB down from the maximum power observed. Similarly, the colour scale shows dB down normalized to maximum.

arriving, especially for low SNR events, which better constrains the inversion for event location and origin time. Additionally, incorporating the estimated angle of incidence into the inversion (with appropriate error bounds) further constrains location reducing uncertainties (error ellipses).

Figure 4 illustrates the optimal three dimensional (3D) alignment vector resulting from the FK (frequency wavenumber) grid-search across the limited 3D slowness domain. The optimal 3D vector listed in the lower left of the Figure and indicated by the maximum of the dark red 'bullseye' in the image reveals slowness and angle of the optimal beam MRA. The shape of the 3D slowness response is a function of several factors including the angle of incidence and wavelength of the incident seismic energy relative to the geometry of the volumetric array.

Processing

The event processing workflow includes data preconditioning (e.g., windowing, filtering, FK beamforming), 4D scanning (event detection), relocation, and moment magnitude calculations. Observed energy of a typical microseismic event arrives first as P-wave energy across the whole network. Figure 5 demonstrates the SNR improvement by taking advantage of the phased array and constructing the optimal beam at each array. This allows low SNR arrivals to be detected and picked more precisely. In addition, by running a full-waveform source scanning (Kao and Shan, 2004) over time and space (e.g., 10m x 10m spatial grids and 5-sec sliding time window) using the whole array network and travel-time look-up-tables, potential events emerge with high semblance (stack of model-aligned energy transient/onset, e.g., STA/LTA). Events above a threshold become the initial set of detected events. Each initial detection comes with a best-matched grid point in space and serves as the initial location input for a relocation process based on an iterative non-linear inversion using the arrival-time picks and optional FK attributes (e.g., azimuth). In addition to a standard least squares location algorithm, velocity model error is further accounted for via Progressive Multiple Event Location (PMEL, Pavlis and Booker, 1983), which simultaneously solves for all event locations and station corrections. This results in more accurate relative locations, but without known ground truth the true velocity model bias remains uncertain. Moment magnitude is calculated by using the displacement spectrum based on the Brune (1970) source model, following Shearer (2009).

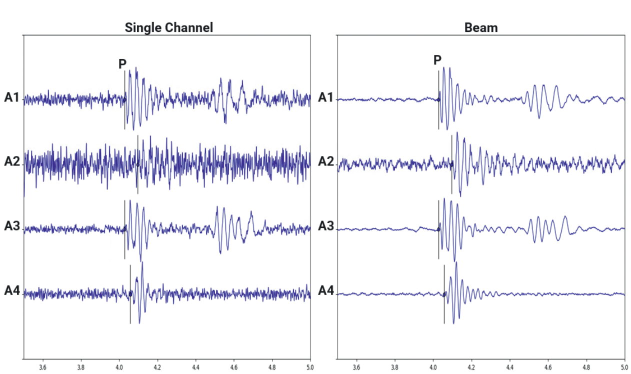

Figure 5 An example event showing dominant arrivals of P waves at each array. Improvement of signal-to-noise ratio is evident by comparing a single channel (left) to the optimal beam (right).

Results

Examples of processing data acquired by the four compact phased arrays installed at the CaMI site are demonstrated by 55 microseismic events spanning nine continuous days taken from the initial bulletin and summarized in Figures 6 through 10. Figure 6 shows a time series (millivolts) and spectrogram (signal power) of a typical microseismic event, in this case observed from the A3 array using the central channel. The first arrivals are P waves with energy above the noise in the frequency range 20-70 Hz, followed in this example by a surface wave. A benefit of the compact phased array is the ability to classify signal wave types using the attributes of FK analysis such as angle of incidence and phase velocity, as well as exploiting the patterns of these attributes in time. Among all the detected events, many have weak signals that are poorly resolved and cannot be reliably picked at any individual sensor without the SNR gain provided by coherently processing the data acquired using the phased arrays (Figure 7). This

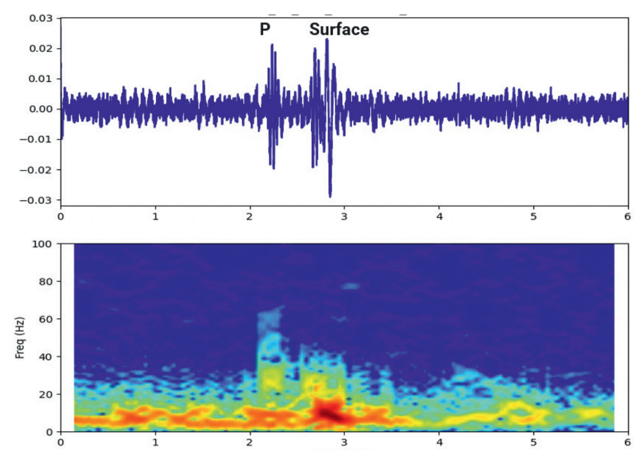

Figure 6 Example taken from the central channel of Array 3 showing weak signals in time domain (top) and spectrogram (bottom). The vertical axis of the time series is amplitude in millivolts, after all data acquisition gains/digitization factors have been removed. The colourmap of the spectrogram is normalized spectral power using a linear scale.

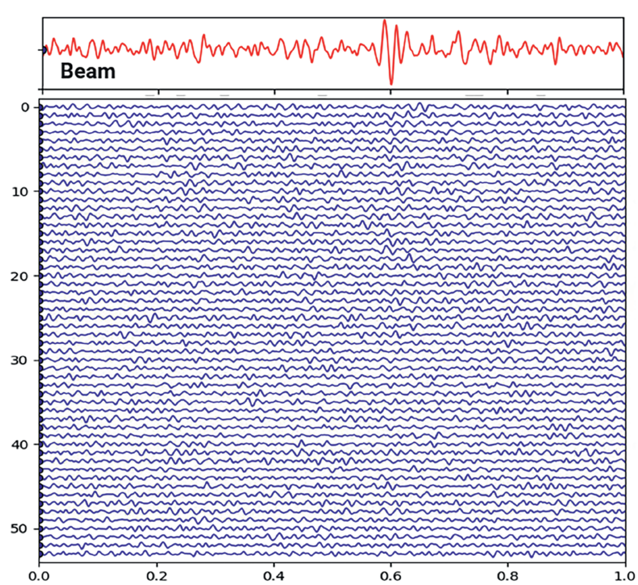

Figure 7 For a typical weak event, seismic signals at individual channels across an array (blue) vs the optimal beam (red) based on array FK analysis.

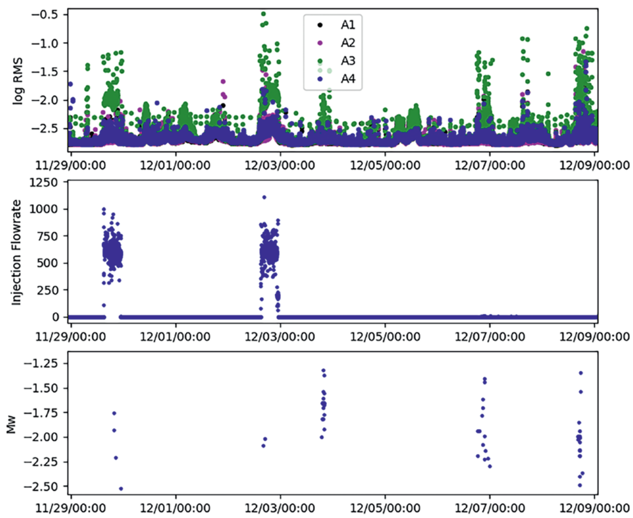

Figure 8 Example of continuous monitoring revealing 55 events within a nine-day period, having a range of M_W=[-2.5, -1.3] (bottom). Seismic events were detected during both injection ON and OFF periods as indicated, compared to the recorded injection flowrate (bottom) . The mean RMS of recorded data at each of the four arrays (top) indicates a correlation of some seismic events with industrial activities not related to injection (bottom, dates 12/04, 12/07, and 12/09).

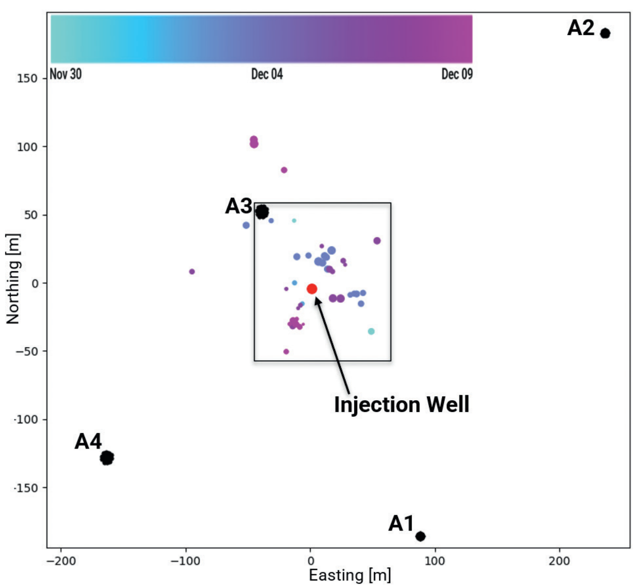

Figure 9 Map view of PMEL locations of the 55 events during reporting period, sized by moment magnitude and colour-coded by date. The box shows the area of focus shown in Figure 10.

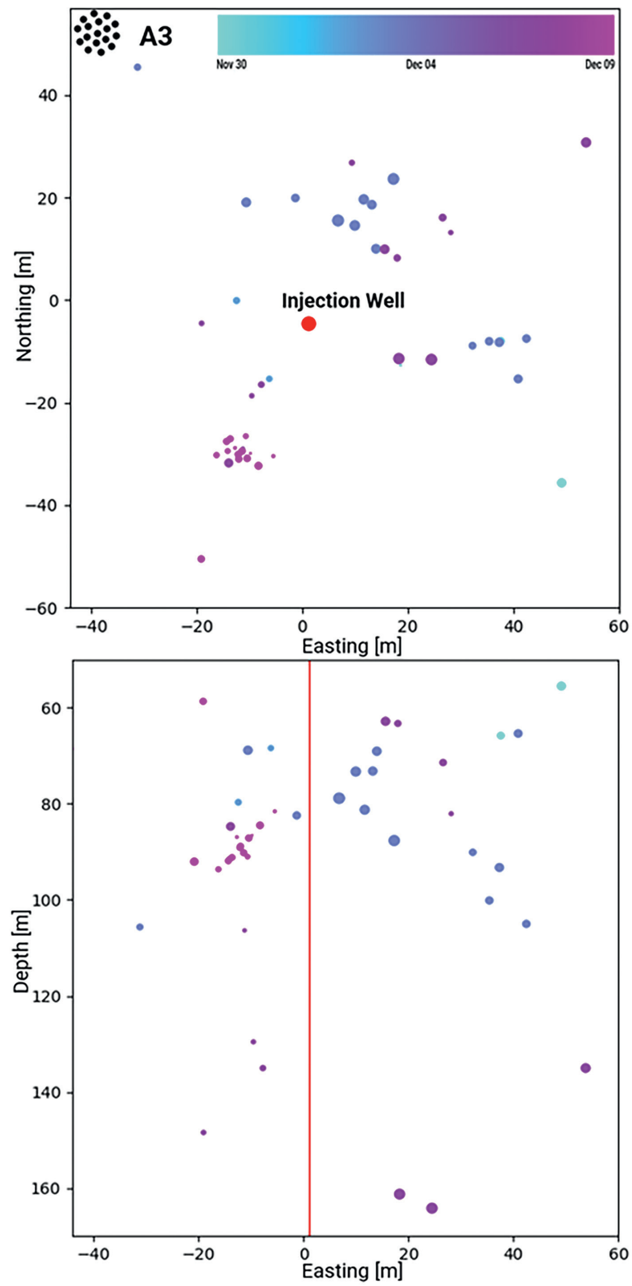

Figure 10 Top: Map view of the events occurring near the injection well (red circle). Bottom: Cross-section view looking north. The vertical red line is the injection well. Events are sized by moment magnitude and colour-coded by date.

observation suggests better performance of the compact arrays compared to a traditional surface network that suffers lower signal levels at large event-sensor offsets and higher noise levels. Savard et al. (2020) observed that P-wave energy is typically absent/undetected at the same site from a 2D surface network.

The 55-event subset spans a moment magnitude range between −2.5 and −1.3 (Figure 8). Events tend to cluster in time during both ON and OFF times of the CO_2 injections. In addition to the injection activity, microseismicity appears to correlate with the data RMS peaks shown in Figure 8 (top) leaving additional potential triggering activities/mechanisms to be considered. Given the precision of the P-wave arrival time picks due to the improved SNR from beamforming, the PMEL relocation of the events allows location uncertainty to be less than 30 m in a relative location context. The result (Figures 9 and 10) clearly shows a spatial clustering with earlier events mainly developed north and east of the injection well then later focused southwest of the well. It is also noted that the majority of the events occurred in the overburden at depths between 50m and 100m (Dinosaur Park formation), which agrees with previous studies on the site (Savard et al., 2020) in which these events are interpreted to be caused by changes in stress in the overburden during increase and relaxation of pressure in the injection zone (300 m depth). As seen in Figure 10 (e.g., magenta-coloured cluster in southwest quadrant of top plot), PMEL relocation focusing on event clusters allows fine structures to be revealed.

Summary and discussion

Quantum Technology Sciences has installed a network of four compact volumetric phased arrays (SADAR arrays) for persistent monitoring of seismicity at the CaMI Field Research Station yielding a number of noteworthy results. The proof-of-concept system features three different permanently installed array designs varying in aperture and depth.

The data from the SADAR arrays are coherently processed generating significant SNR improvements. The increased SNR of array beams, compared to that of individual elements, reduces the uncertainty in determining the phase arrivals and produces better-constrained locations. Coherent processing of the phased array data demonstrates superior phase detection capabilities compared to previous results reported by other studies using surface arrays deployed at the CaMI Field Research Station.

The subset of detection and location results from the bulletin presented here indicate that events tend to cluster in time whether during known CO_2 injection periods or at other times not correlated with injections. Furthermore, the data acquisition and workflow results demonstrate robust detection and location of microseismic events down to $M_w = -2.5$. Ongoing work includes updating the event bulletin, improving the processing workflow aimed at reducing the thresholds for signal detection, utilizing ground truth information in event location, and determining the minimum network and array configuration for computing moment tensor solutions.

While a primary goal of passive seismic monitoring is to better understand geologic reservoir dynamics over the life of the field, understanding the real-time reservoir response aids in quantifying the effectiveness of reservoir engineering actions as well as recognizing potential and incipient problems not directly related to reservoir horizons. The initial results of this compact volumetric array deployment suggest that effective subsurface monitoring may not require a large channel count and wide aperture surface networks nor deep borehole seismometers. A reduced network footprint is more economical to deploy and maintain. We expect system performance will improve with array and network design improvements, including additional benefits from processing multi-component vector sensors emplaced for array elements. Nevertheless, even the limited results presented here demonstrate the performance gains attainable using a network of permanently deployed, compact volumetric phased arrays for monitoring microseismicity associated with geologic reservoirs. Persistent monitoring technologies such as demonstrated here, when fully automated to produce real-time event bulletins, will be an enabling capability for managing gigatonne CO_2 geologic sequestration.

Acknowledgements

Quantum Technology Sciences, Inc., is a wholly owned subsidiary of Geospace Technologies Corporation, Inc. We acknowledge CMC for providing access to the CaMI Field Research Station to enable installation of the SADAR system. The Field Research Station is supported by funding from the Global Research Initiative at the University of Calgary from the Canada First Research Excellence Fund and from the CaMI Joint Industry Project. CMC is also acknowledged for providing operational data from the site.

References

Abraham, D. [2019]. Underwater Acoustic Signal Processing: Modeling, Detection, and Estimation. Springer Nature Switzerland, Cham.

Brune, J. [1970)] Tectonic stress and the spectra of seismic shear waves from earthquakes, JGR, 75,4997.

Nyffenegger, P.A., Tinker, M.A. and Endress, A.O. [2015]. Systems and methods for acquiring and characterizing time varying signals of interest (U.S. Patent No. 09,057,796). U.S. Patent and Trademark Office.

Davis, R.T., Nyffenegger, P.A. and Johnston, K.B. [2015]. Methods for identifying a signal of interest and for making a classification of identity (U.S. Patent No. 09,091,780). U.S. Patent and Trademark Office.

Davis, R.T., Nyffenegger, P.A, Tinker, M.A., Volk, J.M., Johnston, K.B. and Richards, P.T. [2017] Systems and methods for acquiring and characterizing time varying signals of interest (U.S. Patent No. 09,678,231). U.S. Patent and Trademark Office.

Douglas, A. [2013] Forensic Seismology and Nuclear Test Bans. Cambridge University Press, New York.

Havskov, J. and Alguacil, G. [2006]. Instrumentation in Earthquake Seismology. Springer, Dordrecht.

Kao, H. and Shan, S.-J. [2004] The source-scanning algorithm: mapping the distribution of seismic sources in time and space, *Geophysical Journal International*, **157**(2), 589-594.

Lawton, D.C., Dongas, J., Osadetz, K., Saeedfar, A. and Macquet, M. [2019]. Chapter 16: Development and Analysis of a Geostatic Model for Shallow CO_2 Injection at the Field Research Station, Southern Alberta, Canada. in: T. Davis, M. Landrø, and M. Wilson, (eds.) Geophysics and Geosequestration. Cambridge University Press, p.280-296. DOI 10.1017/9781316480724.017.

Macquet, M., Lawton, D.C., Saeedfar, A. and Osadetz, K.G. [2019]. A feasibility study for detection thresholds of CO2 at shallow depths at the CaMI Field Research Station, Newell County, Alberta, Canada. Petroleum Geoscience 25, no. 4. 509-518. https://doi.org/10.1144/petgeo2018-135.

Pavlis, G. and J. Booker [1983]. Progressive multiple event location (PMEL), Bull. Seism. Soc. Am., 73, 1753-1777.

Savard, G., Gilbert, H., Macquet, M., Lawton, D. and Gu, J. [2020]. Microseismic monitoring at a shallow injection site, the CaMI Field Research Station in Newell County, AB. Geoconvention 2020 Virtual Event Conference Processing.

Schweitzer, J., Fyen, J., Mykkeltveit, S., Gibbons, S. J., Pirli, M., Kühn, D. and Kværna, T. [2012]. Seismic Arrays. - In: Bormann, P. (Ed.), New Manual of Seismological Observatory Practice 2 (NMSOP-2), Potsdam: Deutsches GeoForschungsZentrum GFZ, 1-80. https://doi.org/10.2312/GFZ.NMSOP-2_ch9.

Shearer, P. [2009]. Introduction to Seismology, Cambridge University Press, New York.

Tinker, M.A., Nyffenegger, P.A. and Richards, P.T. [2019]. Systems and methods for acquiring and characterizing time varying signals of interest (U.S. Patent No. 10,401,513). U.S. Patent and Trademark Office.

Tinker, M., Hutchenson K., Nyffenegger, P.A, Engelhardt, K. and Lowther, R. [2021] Networked system and method for passive monitoring, locating or characterizing activities (Application submitted to U.S. Patent and Trademark Office).